journal

J. Am. Ceram. Soc., 77 [1] 73–80 (1994)

Coating Additives for Improved Mechanical Reliability of Optical Fiber

Vincenzo V. Rondinella* and M. John Matthewson*

Fiber Optic Materials Research Program, Department of Ceramic Science and Engineering, Rutgers University, Piscataway, New Jersey 08855

Charles R. Kurkjian*

AT&T Bell Laboratories, Murray Hill, New Jersey 07974

Fused silica glass is subject to delayed failure, i.e., failure occurring after a certain time under stress conditions far below the level required to have fast, catastrophic rupture. While the behavior at high applied stress may be described, at least empirically, by the subcritical crack growth model, it is well known that fused silica shows a transition, or "knee," to a more severe delayed failure behavior, or "enhanced fatigue," at low applied stress and long time to failure. This makes predictions of the expected lifetime unreliable. The addition of nanosized particles of fumed silica to the polymer coating of fused silica optical fiber is shown to improve long-term mechanical properties of the fiber: it delays the onset of the fatigue transition and reduces the strength degradation due to zero stress aging. Atomic force microscopy analysis shows that the presence of the additive dramatically reduces the rate of development of surface roughness, thus indicating that the effect of the additive is to suppress surface dissolution processes. The additive has little effect on the fatigue behavior before the transition. These results indicate that dissolution is the cause of the transition but has less importance on the pre-transition region.

I. Introduction

FUSED silica optical fiber is now widely used in many applications; in particular, there are currently in excess of 10^7 km of fiber installed in long-haul telecommunication systems in the United States. In these applications the fiber is frequently exposed to corrosive environments that can cause strength loss, fatigue, and eventual failure. The mechanical reliability of fused silica optical fiber is therefore an important issue, since failure of the fiber can be extremely disruptive and expensive to repair because of inaccessibility of the fiber cable, particularly of submarine cable.

Silica optical fiber, like many other ceramic materials, exhibits fatigue behavior, i.e., failure can occur after a prolonged time when the fiber is subject to a constant applied stress lower than the initial strength; the failure eventually occurs by fast crack propagation.[1]

While it has been argued that the subcritical crack growth model is not applicable to "pristine," high-strength (>5 GPa) fused silica optical fiber because of the absence of initial defects (e.g., Matthewson and Kurkjian[2]), short-term data do empirically fit the model reasonably well[3] although the details of the appropriate chemical kinetics model are not known.[4,5] Therefore, it is tempting to use the model to extrapolate short-term data to in-service lifetimes. However, it has now been well established in several laboratories that under more aggressive fatigue conditions an abrupt transition (or "knee") to the so-called "enhanced fatigue" behavior can be observed at long times to failure and low applied stresses. The knee has been observed for both bare[6] and polymer-coated fiber.[2,6–11] While this result for bare fiber indicates that the transition is not an effect due to the coating, it is known that certain coating parameters, such as adhesion, can influence the fatigue behavior of the fiber.[12,13] Michalske *et al.*[14] point out that if the crack growth kinetics show an exponential dependence on stress, rather than the simple power law, the log–log fatigue plot would show curvature in the same direction as the knee. However, this does not explain the presence of the knee since replotting fatigue data exhibiting the knee (and in particular the data presented here) on semilog axes does not straighten the curve; the knee is too abrupt to be explained away by saying the power law is inappropriate—the transition is real and is likely due to a change in fatigue mechanism. Matthewson and Kurkjian[2] presented results for polymer-coated fused silica fiber that show the presence of a "knee" in the residual strength of fiber subject to zero stress aging. They found that the knees in fatigue and zero stress aging experiments occurred at similar times and concluded that surface corrosion phenomena may be responsible for the enhanced fatigue behavior. This is further evidence that the fatigue knee is a reality and is not an artifact of the crack growth kinetics model used to interpret the data.

For most ceramic materials, the well-known subcritical crack growth model,[1] which involves crack propagation by bond rupture, is accepted as the fatigue failure mechanism.[15,16] However, we shall now review dissolution or material removal as a possible mechanism for strength degradation.

Hillig and Charles considered a model based on differential stress-enhanced chemical corrosion acting preferentially at the tip of a long elliptical surface flaw.[17] They suggested that weakening occurred predominantly by flaw sharpening rather than extension. Chuang and Fuller[18] recently reexamined the model in more detail and included the complete crack geometry, and not just the crack tip, in their analysis of possible shape changes of a flaw. The Charles–Hillig model is now not considered directly applicable to materials with macroscopic flaws since any blunt flaw will sharpen to atomic dimensions and then can only become more severe by extension. However, pristine silica fiber does not have macroscopic cracks, so that whatever flaws are present are already of atomic dimensions in both width and length. Therefore, changes in the flaw geometry can be important in determining the evolution of the flaw and the strength loss of the fiber. Kurkjian, Krause, and Paek[19] proposed a pit etching model in which blunt pits are developed in the surface of the silica to explain the zero stress aging behavior. Yuce and co-workers have measured surface roughness of silica fiber using scanning tunneling microscopy[20] and atomic force

T. Michalske—contributing editor

Manuscript No. 194711. Received April 1, 1993; approved August 3, 1993.
Presented at the 94th Annual Meeting of the American Ceramic Society, Minneapolis, MN, April 15, 1992 (Glass and Optical Material Division, Paper No. 3-JXVI-92).
*Member, American Ceramic Society.

microscopy (AFM)[21] and have shown that the roughness increases dramatically with prolonged exposure to an aggressive environment. They found that the residual strength after zero stress aging closely correlates with the magnitude of the surface roughness, with increasing roughness giving decreasing residual strength. These results were sensitive to the environment and to the nature or absence of a polymer coating. Most of these results correspond to the posttransition behavior; therefore, it seems likely that the mechanism giving rise to the fatigue knee involves surface dissolution to form pits, which then act as stress concentrators and can be thought of as flaws from which cracks can initiate under the application of stress. Inniss *et al.*[22] found that the strength of silica surfaces etched in HF vapor could be predicted from the shape (both depth and width) of the discrete pits observed using AFM. Taken together, all these results strongly suggest a causal relationship between surface roughness and strength degradation.

Recent work has shown that surface phenomena play an important role in determining the fatigue behavior of pristine silica fiber. Matthewson, Rondinella, Lin, and Keyes[23] have reported dynamic fatigue results that show an alkali cation dependence of the strength of silica fiber in aqueous solution at high pH that closely correlates with dissolution rates in the same environments. This led the authors to suggest that dissolution may also be important on a short time scale. However, the results presented here do not support this hypothesis.

The various results discussed above indicate that the mechanism for the fatigue knee is surface roughening to produce stress concentrating pits and that the roughness is caused by dissolution. This observation further implies that reduction of the rate of dissolution will have a beneficial effect on fatigue and long-term reliability. There are several ways of interfering with the chemical reaction between silica and water: for example, by decreasing the pH or by adding third components that change the equilibrium conditions. Perhaps the most obvious way of slowing dissolution is to add the product of dissolution to the environment. We have performed some preliminary experiments in which bare fibers were fatigued in dilute solutions of silicic acid. However, at the elevated test temperatures required to obtain the fatigue transition on a reasonable time scale, the solutions were prone to gelation. The dissolution processes of silica are complex in that the product of dissolution, silicic acid, subsequently oligomerizes and polymerizes.[24] It is therefore not clear what the effective concentration of the silicic acid was in these experiments. For this reason, even though those experiments are of a more fundamental nature, they have been postponed in favor of a more practical approach. This paper describes the results of this approach to the problem, which involves incorporating fine silica particles in the polymer coating of a coated fiber. The original assumption was that these particles would dissolve and would become a source of silicic acid.

The polymeric coatings normally applied to silica fiber act primarily as a protective barrier against mechanical abrasion. However, polymer coatings are not hermetic and they are relatively permeable so that mobile species can diffuse through and react with the fiber surface. While the coating impedes diffusion of mobile species to the silica surface, it also slows down the diffusion of the reaction products away from the surface. It defines, at the glass/coating interface, a local environment that may differ from the nominal conditions outside the coating.[2] It is well known that if the fiber is stored in one environment and tested in another, sufficient preconditioning time must be allowed in order to chemically "equilibrate" the glass surface of the fiber with the test conditions, as demonstrated by Rondinella and Matthewson.[25]

In the present work the polymer coating of fused silica optical fiber is used as a source of silica more readily available to interact with the diffusing environment than the molecules on the surface of the glass. The results presented here show the effect of the addition of colloidal silica particles to the coating on the mechanical properties of the fiber. Dynamic fatigue, static fatigue, and zero stress aging experiments have been performed. These results, if compared with the same silica fiber without any additives in the coating, show a systematic improvement of the post-aging strength and the resistance to enhanced fatigue. Direct observations of the glass surface after zero stress aging have been used to correlate the strength and surface roughness and to establish the importance of dissolution as a mechanism for the fatigue transition.

II. Experimental Procedure

(1) Fiber Fabrication

Two lengths of fiber with a 125-μm glass diameter and ~250-μm outer polymer diameter were drawn from the same fused silica preform and coated in-line with two different coatings: the first length was coated with a UV-curable acrylate (designated "without" fiber); the second length was coated with the same polymeric coating material, to which ~0.7 wt% of fumed silica powder had been previously added to the liquid prepolymer (designated "with" fiber). The "without" fiber acts as a control for comparison to the "with" fiber. Since the two fibers were drawn from the same preform under identical conditions and with coating material from the same batch, any difference in behavior can only be attributed to the presence of the silica in the "with" coating. The powder used was Cab-O-Sil M5 which has particle diameters in the range of 5 to 30 nm and a surface area of ~200 $m^2 \cdot g^{-1}$.[26] Although the additive was only 0.7 wt%, the total surface area of the silica particles was calculated to be on the order of 100 times the surface area of the fiber for a given length of fiber. Such small particles are appreciably more soluble than a flat surface. The combination of large surface area and higher solubility means that the additive molecules are considerably more available for reaction with water than the fiber surface molecules.

The silica powder was mixed with the coating prepolymer by manual stirring. The mixture was held at a temperature of ~50°C for several hours in order to remove the air bubbles formed during mixing. This step was performed in a dark box to avoid premature curing of the coating by UV radiation from laboratory light sources. At the end of this process, the coating material appeared cloudy, indicating that the particles were not fully dispersed.

After drawing, the fibers with the two coatings were distinguishable. The "with" fiber coating had a bumpy outer surface, while the "without" fiber coating surface had the usual smooth aspect. This difference is probably due to the somewhat higher viscosity of the "with" coating prepolymer, which affects its behavior during the coating process; this process is optimized for the untreated "without" prepolymer. The uniform coverage of the glass surface by the coating for the "with" fiber was checked and no pinholes were detected.

(2) Test Methods

Static fatigue experiments have been performed on "with" and "without" fiber using a two-point bending technique. Figure 1(a) is a schematic of the apparatus[27] in which a short length of fiber is bent inside a precision-bore glass tube. The peak strain, ε, occurring on the surface of the fiber at the tip of the bend is given by[28]

$$\varepsilon = \frac{1.198 d_f}{D - d_c} \tag{1}$$

where D is the diameter of the tube, d_f is the diameter of the glass fiber, and d_c is the overall outer fiber diameter, including the coating. The applied stress, σ, is then calculated by

$$\sigma = E(\varepsilon)\varepsilon \tag{2}$$

where $E(\varepsilon)$ is Young's modulus. $E(\varepsilon)$ is strain dependent, and is given by

$$E(\varepsilon) = E_0(1 + 3.2\varepsilon + 8.48\varepsilon^2) \tag{3}$$

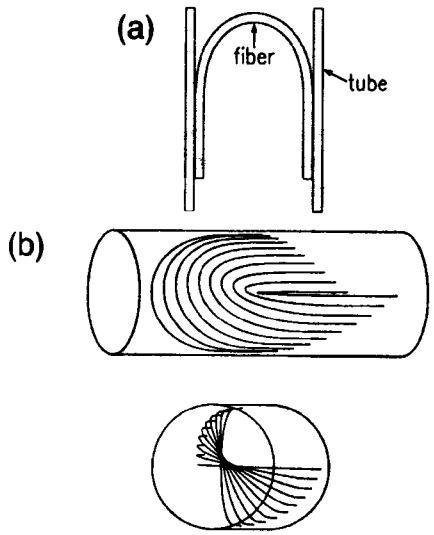

Fig. 1. Schematic of how fiber loops are placed in precision bore tubes for static fatigue experiments in two-point bending: (a) shows the shape of the bent fiber and (b) shows how many fibers can be inserted into the tube and tested simultaneously.

where E_0 is the zero strain modulus of 72.2 GPa. The numerical coefficients in Eq. (3) are calculated from the results of Krause, Testardi, and Thurston.[29] Tubes with a range of diameters have been used that give a useful range of bending stresses. The same applied stress values, i.e., the same tube diameters, have been used for both types of fiber. Using this technique, many samples can be tested simultaneously under identical environmental and stress conditions; in this work, 25 specimens were loaded in each tube (Fig. 1(b)). After the specimens are loaded, the tubes are immersed in the test environment. The break of each specimen is detected acoustically by a transducer connected via a trigger circuit to a chart recorder or other suitable monitoring device. The time to failure can be easily derived from the position of each break signal on the chart. For the present work, pH 7 phosphate and pH 10 carbonate–borate buffer solutions were used as test environments to evaluate the influence of pH. The fatigue tests were accelerated by using a temperature of 90°C, so that the fatigue transition was occurring on a relatively short time scale (approximately 24 h for the pH 10 environment).

Zero stress aging experiments have also been performed, in which samples of both fibers were aged unstressed in the test environments for various times; 50 specimens of each fiber were used for each aging time. After aging, the residual strength and the fatigue parameter, n, of the two types of fiber were measured using a modified dynamic two-point bend strength test. This test constitutes the dynamic analogue of the static experiment described above in which the fiber is bent between two grooved faceplates which are then brought together by a computer-controlled stepper motor.[28] The breaks are detected acoustically and the stress to failure, σ_f, can be calculated from equations similar to Eqs. (1), (2), and (3); in this case, D is given by

$$D = d + d_g \tag{4}$$

where d is the faceplate separation at failure and d_g is the total depth of both grooves. For the present work two slightly different versions of the apparatus have been used. The first is for coated fiber; the faceplates have 10 accurately machined grooves, making it possible to test up to 10 samples simultaneously. Grooved faceplates are unsuitable for measurements on bare fiber because the unavoidable roughness inside the groove damages the fiber surface. Therefore, a second version of the apparatus has been used in which the bare fiber is balanced between polished faceplates;[30] the strain (or the stress) is then calculated via Eq. (4) with $d_g = 0$.

The residual strength of the aged specimens was measured at room temperature while immersed in the same environment in which the aging was performed. The strength was measured at four different faceplate velocities (1000, 100, 10 and 1 $\mu m \cdot s^{-1}$, respectively) in order to determine the dynamic fatigue behavior. Typically, 10 samples were used for each faceplate velocity. The value of the stress corrosion susceptibility parameter, n, can be calculated from the slope of log–log plots of stress to failure, σ_f, versus faceplate velocity, v.[28] A representative average strength was determined from each dynamic fatigue plot by interpolating the linear regression fit (and its confidence intervals) to the central speed of 32 $\mu m \cdot s^{-1}$. This gives a more accurate estimate of the representative strength than simply averaging 10 measurements at a single speed. Furthermore, it gives smaller estimates of the error in the mean strength than averaging all 40 measurements, which would introduce artificial scatter because of the fatigue effect. This technique, therefore, efficiently uses information from measurements at all speeds, while factoring out the variation in strength with fatigue.

The fatigue parameter, n, is normally defined from fatigue data that quantify the strength by the failure stress. Therefore, all the strength data presented here are in terms of stress to failure (see the discussion in Ref. 25). All of the dynamic fatigue data obtained using two-point bending have been corrected to compensate for small laboratory temperature fluctuations using a reference temperature of 22°C.[23]

III. Experimental Results

(1) As-Received Strength

The strength and dynamic fatigue of the as-received, unaged fiber were measured in order to determine whether the addition of silica to the coating has a detrimental effect on the short-term mechanical behavior. Figure 2 shows dynamic fatigue data in two-point bending for unaged bare fibers (solid symbols) whose coating material had been removed prior to testing by briefly dipping in hot (~200°C) sulfuric acid with a subsequent rinse in acetone and deionized water. The fiber was tested at room temperature, immersed in pH 7 buffer solution in order to control the pH and the water reactivity. These particular experiments were performed at constant stress rates[31] of 700, 70, 7, and 0.7 $MPa \cdot s^{-1}$ rather than at constant faceplate velocity. Rondinella and Matthewson[25] showed that the two loading modes give the same values for the fatigue parameters. Each point represents the average for 10 specimens and the error bars correspond to a 95% confidence interval on the mean. The data for the "with"

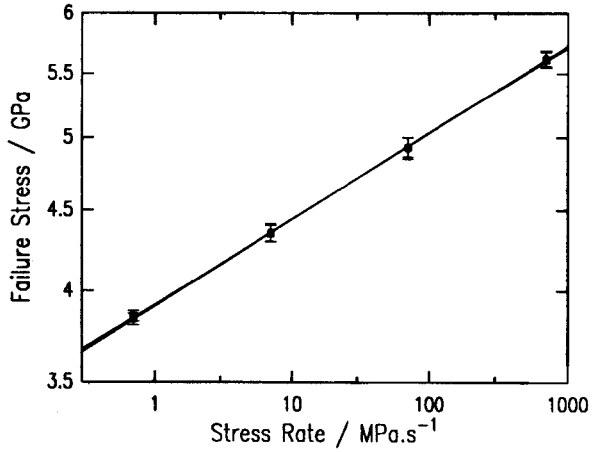

Fig. 2. Dynamic fatigue behavior of bare fiber with (■) and without (●) silica particles added in the coating.

and "without" fiber are indistinguishable, showing that the initial strength of the glass for both coatings is the same, and therefore the addition of silica in the coating does not damage the glass surface on a short length scale.

Figure 3 shows the results of a similar experiment performed on coated fiber at constant faceplate velocities of 1000, 100, 10 and 1 $\mu m \cdot s^{-1}$. In this case the fibers were presoaked in pH 7 buffer solution for at least 24 h in order to equilibrate the fiber with the testing environment. These data do show a small difference between the "with" and "without" fiber, with n values of, respectively, 19.39 ± 0.68 and 20.03 ± 1.69 and mean strengths of 5.328 ±0.002 and 5.440 ± 0.006 GPa. The n values of "with" and "without" appear practically indistinguishable. It cannot be excluded that a slight weakening effect on the "with" fiber may occur, due to the mechanical interaction of the silica particles with the glass surface during the bending test. However, it should be noted that the error bars for all the points overlap.

While the silica additive has little effect on the bending strength, two-point bending only tests an effective length of approximately 20 μm.[30] It is therefore possible that the additive could produce only occasional defects that are less likely to be encountered in bending. For this reason, the tensile strength of the two types of fiber was measured in ambient air (20% relative humidity) at a loading rate of approximately 500 $MPa \cdot s^{-1}$ and with a 15-cm gage length. Ten samples for each type of fiber were broken. The average strength for "without" fiber is 5.55 ± 0.03 GPa, while for the "with" fiber it is 3.22 ± GPa, with Weibull moduli of 74 ± 44 and 5 ± 3, respectively. This observation shows that the addition of silica can damage the fiber, either before or during the tensile test.

The unaged strength results indicate that the intrinsic, initial strength of the glass is the same for the two types of fiber, and is not affected by the process of applying the coating. However, occasional weak spots appear to be present on the "with" fiber, and are detectable by testing longer lengths of fiber. It is possible that these weak spots are due to mechanical damage on the glass surface caused by the silica particles occurring during the test. Since a nanosized particle is unlikely to significantly damage the fiber surface, it is probable that hard, large agglomerates of silica particles are responsible for the damage. This is supported by the observation of cloudiness in the prepolymer mentioned in Section II(1). This problem can probably be eliminated with the adoption of a more sophisticated process control for the mixing and dispersion of the additive in the coating prepolymer.

(2) Static Fatigue

Figure 4 shows the static fatigue data for both "with" and "without" fiber at 90°C in pH 7 buffer solution. Each point typically represents the average time to failure of 25 specimens and the error bars correspond to a 95% confidence interval on the mean. At short times to failure both fibers give similar results. This convergence is an artifact of this particular implementation of the two-point bending technique, since the specimens are immersed in the environment at time zero and cannot be preequilibrated. Matthewson and Kurkjian[2] found that differences in failure times in different pH environments at 90°C were observable only after ~20 min, which is therefore the time it takes the chemical nature of the environment to penetrate the coating. Differences between the two fibers are not expected to be observed on time scales shorter than this. Both sets of data exhibit a pronounced "knee" or transition that is not removed by replotting on semilogarithmic axes. This means that the transition is not an artifact of using a power law crack growth kinetics model instead of an exponential,[14] but is a real effect. The onset of the fatigue transition occurs at about 10^4 s for the "without" fiber and is significantly pushed out in time, to approximately ~3 × 10^5 s, for the "with" fiber, with a significantly more abrupt change in slope after the transition.

At lower stresses the two curves become closer again, but throughout the posttransition region the "with" fiber has a lifetime ranging from 3 to 30 times longer than the "without" fiber. This represents a substantial improvement in reliability for the "with" fiber at low applied stress.

It is noted that the "with" fiber exhibits significantly more scatter in the time to failure than the "without" fiber, particularly in the posttransition region. This is caused by the presence of a few relatively weak specimens in the "with" sets of samples. Figure 5 shows Weibull plots for "with" fiber samples at two representative applied stresses: 2.5 GPa corresponding to the pretransition region and 1.95 GPa corresponding to the posttransition region. The first sample was composed of 47 specimens and the second of 49. The posttransition behavior is clearly bimodal, with, in this case, perhaps 10 specimens in the low tail of the time to failure distribution. While all the "with" fiber data are bimodal in the posttransition region, all of the "without" data are unimodal in this region. Both types of fiber exhibit unimodal behavior in the pretransition region. The low and high strength mode data of Fig. 4 for the "with" fiber have been analyzed separately and are shown in Fig. 6. For comparison, the sketched fit to the "without" data shown in Fig. 4 is also drawn. By eliminating the low strength mode specimens, the scatter in the time to failure of the remaining high strength mode specimens is significantly lowered and is comparable to the scatter for the "without" fiber. Additionally, the mean time to failure is increased, so that the onset of the transition now occurs at nearly two decades further out in time than the "without" fiber.

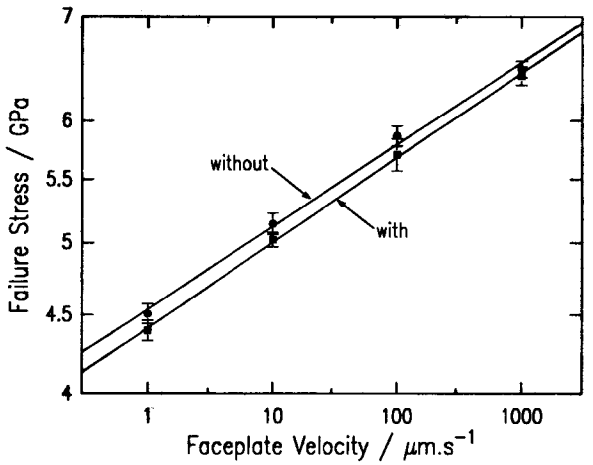

Fig. 3. Dynamic fatigue behavior of coated fiber with (■) and without (●) silica particles added in the coating.

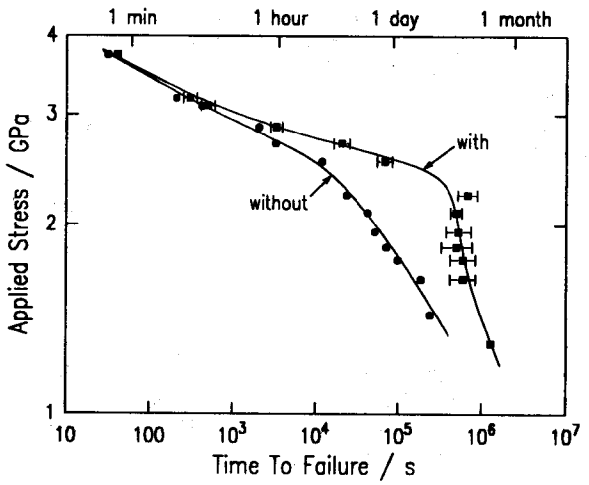

Fig. 4. Static fatigue behavior of the fiber with (■) and without (●) the silica additive in the coating tested in 90°C, pH 7 buffer solution.

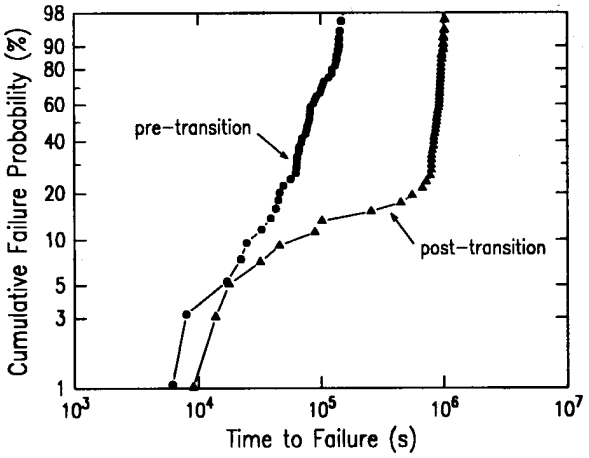

Fig. 5. Weibull plot of the time to failure of "with" fiber subjected to an applied stress of 2.5 GPa (●, pretransition region) and 1.95 GPa (▲, posttransition region). The test environment is 90°C, pH 7 buffer solution.

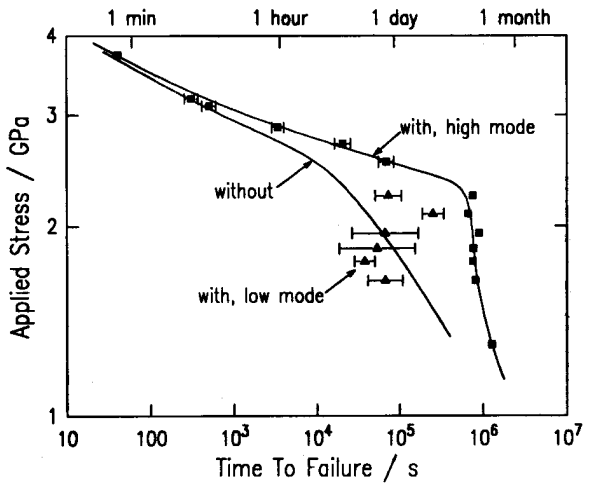

Fig. 6. Data of Fig. 4 after analyzing separately the high (■) and low (▲) strength modes for the "with" fiber. The data points for the "without" fiber have been omitted for clarity, although the sketched line of Fig. 4 is retained for comparison.

The low strength mode data have large error bars because of their small number. Some of the low strength data (about 30% overall) fail at shorter times than any of the corresponding "without" fibers. These specimens presumably suffered some surface damage from abrasion by the coating additive, probably induced when the fibers were loaded into the precision bore tubes. The rest of the low strength data give failure times that are similar to or greater than the "without" fiber. This suggests that much of the weak mode is caused by the already mentioned imperfect dispersion of the silica particles in the coating. This implies that in the "with" coating there are occasional spots essentially silica-free; therefore, if one of these regions coincides with the small portion subjected to significant stress,[27] the fiber specimen will fatigue at the same rate as the "without" fiber. It is expected that with improved preparation techniques the low strength mode can be eliminated.

Figure 7 shows the static fatigue data for "with" and "without" fiber in pH 10 buffer solution. The trends here are similar to the pH 7 data, although the difference between "with" and "without" fiber is smaller in this more aggressive environment.

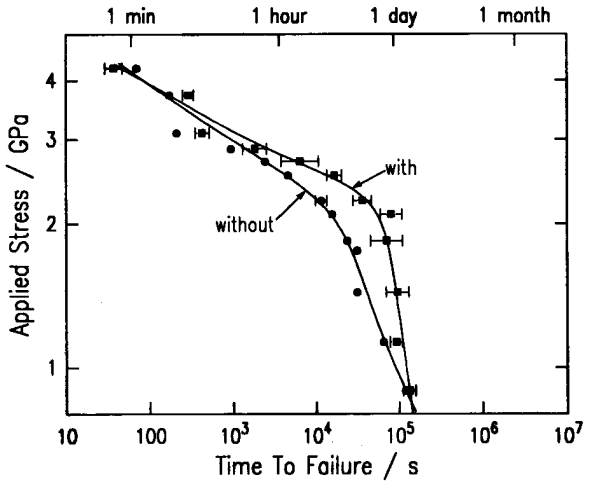

Fig. 7. Static fatigue behavior of "with" (■) and "without" (●) fiber tested in 90°C, pH 10 buffer solution.

Again in the pH 10 environment, the "with" fiber exhibits bimodal behavior in the posttransition region.

It is observed that at the lowest applied stress the times to failure of "with" and "without" fiber coincide. A possible explanation for this convergence is that at very long durations all the silica in the coating of the "with" fiber is dissolved and diffuses out of the coating. It was observed that the coating swelled and fell off during zero stress aging after ~72 h in pH 10 for both types of fiber. This implies that diffusion of dissolved silica through the coating becomes progressively easier with time. The silica certainly does diffuse out of the coating because after about 36 h (in 90°C, pH 10) tenuous clouds are observed in the test solution of the "with" fiber, presumably composed of gelled silica from the coating. When all the silica powder has been dissolved and removed, it gives no extra protection to the fiber so that long duration behavior, at these elevated temperatures, is the same for "with" and "without" fiber. This is supported by the observation that the "with" and "without" behaviors converge more rapidly at low stress in the pH 10 environment, in which silica is more soluble, and by the fact that the cloudiness in the test solution appears later in the case of pH 7. If this mechanism is indeed correct, it implies that a higher starting concentration of silica in the coating would delay the convergence. Therefore, better dispersion of more silica in the coating is expected to further increase the already substantial improvements obtained with the fiber described here.

(3) Zero Stress Aging

The post-aging residual strength has been measured from dynamic fatigue experiments using the two-point bending technique described above. The fibers were broken at room temperature in the same environment in which they were aged in order to avoid concerns of equilibrating the fiber with different environments.

Figure 8 shows the residual strength of fiber after aging in 90°C, pH 7 buffer solution for 0, 12, 24, 168, and 216 h. Except for the initial, unaged strength, the "with" fiber shows consistently higher residual strength after all aging times. It is not possible to identify a clear monotonic time dependence of the residual strength. For the "with" fiber, in particular, after an initial decrease at 12 h, the strength appears to increase slightly with further aging.

Figure 9 shows the residual strength values for both types of fiber after aging in 90°C, pH 10 buffer solution. In this case aging times of 1, 24, 48, and 72 h were used. The coating becomes very soft and viscid with increasing aging time, especially for "without" fiber. Its thickness decreases, but it is difficult to measure it accurately. Eventually, after 72 h at 90°C, the

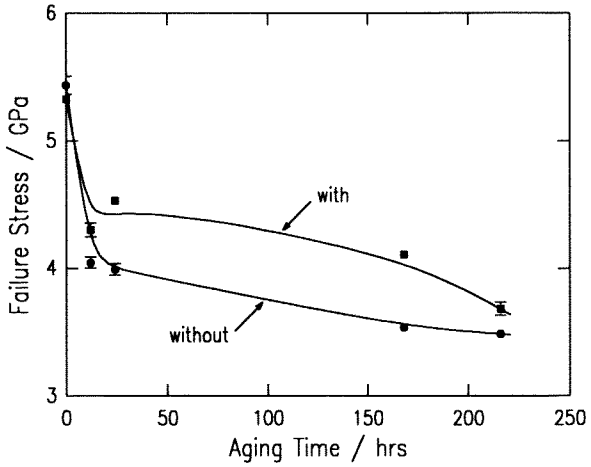

Fig. 8. Postaging strength as a function of aging time for "with" (■) and "without" (●) fiber aged in 90°C, pH 7 buffer solution.

coating slips off from both types of fiber, making the continuation of the experiment pointless.

In the pH 10 environment the residual strength of "without" fiber exhibits more scatter and a nonmonotonic aging time dependence. As in the pH 7 case, however, the "with" fiber is systematically stronger than the "without" fiber.

Besides the residual strengths, the value of the fatigue parameter, n, has been calculated for all of the points in Figs. 8 and 9 and the results are summarized in Tables I and II. No significant differences have been noticed between "with" and "without" fibers, nor any substantial variation with aging time.

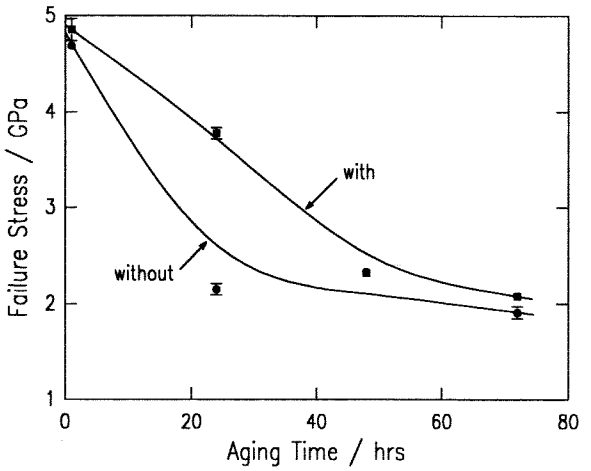

Fig. 9. Postaging strength as a function of aging time for "with" (■) and "without" (●) fiber aged in 90°C, pH 10 buffer solution.

Table I. Values of the Fatigue Parameter, n, for Fiber with and without Addition of Silica Particles in the Coating after Different Aging Times in 90°C pH 7 Buffer Solutions

	n	
Time (h)	Without	With
0	20.0 ± 1.7	19.4 ± 0.7
12	20.2 ± 1.6	18.4 ± 1.8
24	19.3 ± 1.7	17.5 ± 0.7
168	19.4 ± 0.8	17.9 ± 0.2
216	19.2 ± 0.8	19.5 ± 2.2

Table II. Values of the Fatigue Parameter, n, for Fiber with and without Addition of Silica Particles in the Coating after Different Aging Times in 90°C pH 10 Buffer Solutions

	n	
Time (h)	Without	With
1	18.5 ± 0.4	17.4 ± 2.8
24	15.2 ± 2.2	17.6 ± 3.0
48	17.2 ± 0.5	17.4 ± 0.9
72	19.4 ± 4.4	17.2 ± 1.8

(4) AFM Profilometry

Atomic force microscopy (AFM) used for high-resolution surface profilometry has been shown to be an important tool in understanding the mechanisms of strength degradation of high-strength optical fiber.[21,22] This technique has been used to examine the post-aging surface of the "with" and "without" fiber. As for the strength measurements on bare fiber described above, the coating was removed from the aged fiber using 200°C sulfuric acid. A criticism of this method is that it might remove more than the coating, a surface hydrated silica layer, for example. However, Yuce *et al.*[21] found no difference in the surface profiles of unaged fiber after removing the coating by either hot acid or manual stripping of fiber softened by methylene chloride. Furthermore, it should be noted that a hydrated silica surface layer is unlikely to be able to support any significant stress; the strength is expected to be determined by the underlying hard surface. However, since in this study all specimens were prepared in the same way, any differences in the surface profiles (be they of the glass or a hydrated layer) must be due to the presence of the silica additive. All AFM images shown here are on the same scale and have been substantially flattened by computer software in order to remove the curvature of the cylindrical fiber.

Figure 10 shows an AFM image of the glass surface of an unaged fiber; the surface is smooth with a 0.30-nm rms roughness (strength 5.4 GPa). There are no observable differences between the surfaces of unaged "with" and "without" fiber. This agrees with the mechanical test results described in Section III(1), which exhibit the same initial bending strength for both types of fiber. Given that AFM can examine only a small part of the fiber surface, it is unlikely that the kind of defect would be encountered that gives rise to the low tensile strength of the "with" fiber.

Figure 11 shows the AFM image, drawn with the same vertical scale as Fig. 12, of the glass surface of a "without" fiber after aging for 168 h (= 1 week) at 90°C and pH 7. This image shows a dramatic increase in surface roughness (1.36-nm rms roughness) compared to the unaged fiber; the higher roughness

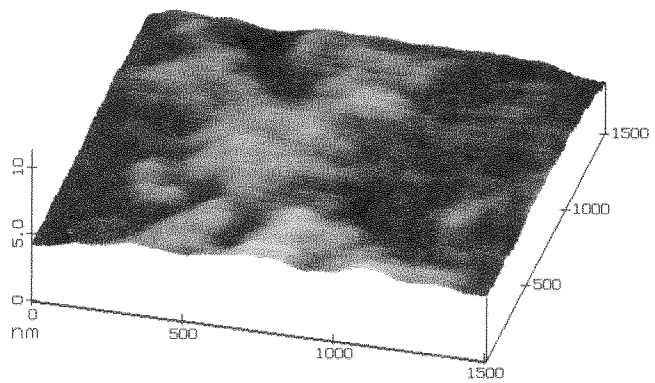

Fig. 10. AFM image of the bare surface of unaged fiber.

is the cause of the lower strength (~3.6 GPa, from an initial strength of ~5.4 GPa).

By comparing the surface profile in Fig. 11 with Fig. 12, which shows the AFM image of a "with" fiber aged under identical conditions (168 h in 90°C, pH 7), a clear indication of the different aging behavior is obtained. The surface in Fig. 12 is significantly smoother (0.46-nm rms roughness) than the one in Fig. 11. This corresponds to a higher residual strength (~4.4 GPa) and confirms that a lower strength corresponds to a higher roughness. Although there is a small difference in rms roughness between the unaged surface of Fig. 10 and the aged "with" surface of Fig. 12, a clear difference in the nature of the roughness is evident. In particular, the wavelength of the surface roughness becomes shorter with the aging treatment.

IV. Discussion

The dynamic fatigue experiments performed using two-point bending show that the two types of fiber, both with and without silica added to the coating, have the same initial strength on a short length scale. In particular, the bare fiber results indicate that the presence of fine silica particles in the coating does not induce any strength loss during the process of fabrication of the fiber. However, the uniaxial tensile tests that involve longer lengths of fiber show that weak spots are present in the "with" fiber. These weak spots are probably caused by the mechanical interaction of hard agglomerates of silica with the glass surface. By obtaining a better dispersion of silica these weak spots should be eliminated. Preliminary results for fiber coated with a polymer that had been filtered through a 20-μm membrane show that filtering substantially reduces the frequency of weak spots.[32]

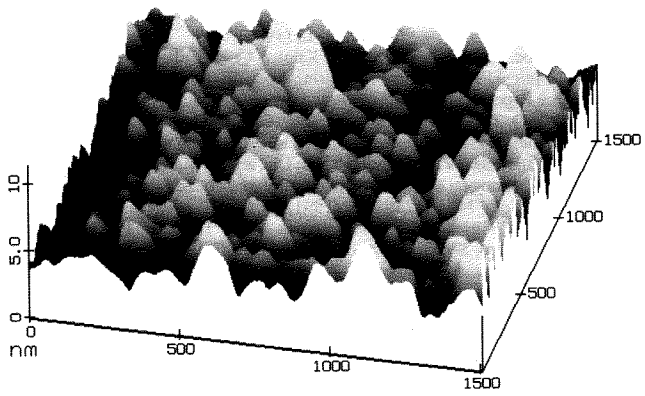

Fig. 11. AFM image of the bare surface of "without" fiber aged 168 h in 90°C, pH 7 buffer solution.

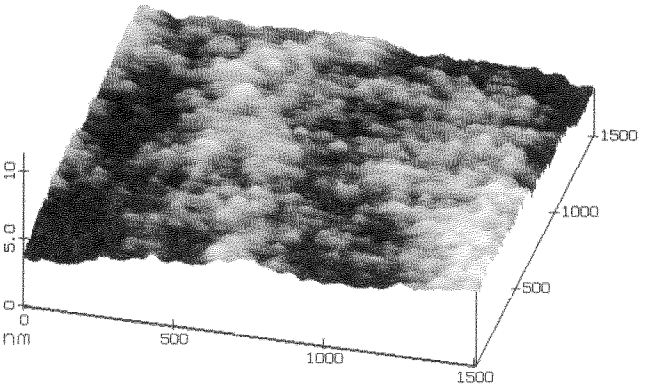

Fig. 12. AFM image of the bare surface of "with" fiber aged 168 h in 90°C, pH 7 buffer solution.

The addition of silica in the coating causes a significant delay in the onset of the fatigue transition, but has little effect on the pretransition region. This indicates that different mechanisms are responsible for the pretransition fatigue of the fiber and the stress-independent, delayed failure behavior of the posttransition region. Moreover, the presence of additive in the coating positively affects the residual strength after zero stress aging. This means that similar mechanisms are responsible for both the posttransition and the zero stress aging behavior of the fiber. These mechanisms are most likely dissolution phenomena, such as roughening, occurring on the glass surface. Direct evidence of these mechanisms is presented by the AFM and STM image analysis both here and elsewhere.[20,21] The decreasing post-aging strength correlates with an increasing roughness, and the presence of silica particles seems to partially inhibit this process. We propose three possible mechanisms which act, either alone or in combination, to improve the aging and fatigue behavior of the fiber:

(1) As water diffuses through the coating to the fiber surface, it dissolves the silica particles and becomes partially saturated. The dissolved silica is then transported to the fiber surface, where it slows the rate of dissolution of the glass surface itself. Diffusion of dissolved silica through the coating does occur with sufficient rapidity for this mechanism to be operative; this is supported by the fact that the silica was observed to diffuse out of the coating during the static fatigue and zero stress aging tests.

(2) Compared to the fiber, the particles have a large surface area and a relatively reactive surface. It is therefore possible that they adsorb reactive species diffusing through the coating, thus lowering the concentration of these species at the fiber surface. However, since the coatings are highly permeable this mechanism is likely to be rapidly saturated.

(3) Silica particles at the fiber surface may protect it in a sacrificial way; reactive species arriving at the surface would preferentially react with particles due to their higher surface reactivity (caused by the high curvature). This mechanism differs from mechanism 1 because it involves silica particles located at the fiber surface and therefore does not involve diffusion of silica through the coating. If, for example, the silica particles were incorporated in an outer polymer coating, with an undoped inner buffer, this mechanism would be inoperative. However, preliminary results[32] from on-going experiments indicate that the presence of silica in the outer layer of a dual coating does indeed extend the lifetime so that this mechanism may not be important.

The presence of an undoped inner coating is also useful because it eliminates any possibility of hard agglomerates of particles damaging the fiber surface, thus improving the tensile strength.

The observation that the "with" and "without" behaviors converge (at least on a logarithmic scale) at long times to failure indicates that the protective function of the additive eventually can be exhausted. However, this observation does not eliminate any of the mechanisms proposed above.

This work does not provide definitive explanations for the measured effects, but does establish their practical significance. Further experiments are required to lend support to a particular model. These include continuation of the preliminary experiments on bare fiber in silicic acid solutions. It is also useful to determine how the strengthening depends on the silica concentration and mobility in the coating. Preliminary results of ongoing experiments indicate that the factor by which the additive improves the lifetime is roughly proportional to the concentration of silica in the coating.[32]

Addition of reactive additives to the coating could have significant applications for other glass fiber systems. For example, heavy metal fluoride fibers (e.g., ZBLAN compositions) have important potential applications for infrared transmission at longer wavelengths than silica. However, the fluorides have poor mechanical properties and durability. In fact, suitable coating additives may have a more dramatic impact on the heavy

metal fluorides since their behavior appears to be effectively posttransition, with a relatively minor sensitivity to applied stress.[33]

If the coating additive is chosen to be a component of the glass fiber, as in this work, several questions need answering. These might include, what components of the glass should be used, what particles sizes are required, and can devitrification of the fiber due to the proximity of crystalline phases be avoided? If these questions can be answered, the approach used in this work should be applicable to a wide range of fiber types.

V. Conclusions

The addition of fine (nanosized) particles of fumed silica to the urethane acrylate coating of silica optical fiber causes significant improvements in the long-term mechanical properties of the fiber. In particular, it delays the onset of the fatigue transition (by nearly 2 orders of magnitude in pH 7), and increases the resistance to strength degradation caused by zero stress aging.

The fatigue behavior of the pretransition region is not significantly affected by the presence of additive in the coating. This indicates that different mechanisms are responsible for the two regions, and that the mechanism responsible for the posttransition region is similar to that involved in the strength degradation after zero stress aging, i.e., dissolution-based surface phenomena.

AFM surface analysis provides some evidence concerning the latter mechanisms: the decrease in strength corresponds to an increase in roughness. The presence of the silica in the coating inhibits the roughening process by partially suppressing the dissolution of the fiber surface. Several mechanisms have been proposed.

There are several fruitful areas for further research. In particular, it should be possible to further improve the performance of silica fiber by optimizing the particle concentration and the dispersion of the particles in the coating. Furthermore, the technique is applicable to any polymer coating material and can potentially provide inexpensive insurance against early onset of the fatigue transition for many types of fiber.

Other substances could be used as additives; any substance that influences the equilibrium between water, silica, and its dissolution products could perform as well as or better than colloidal silica. Moreover, similar additions could be tested for different types of glass fibers, such as multicomponent oxides, nonoxides, etc.

At the moment, reliable lifetime predictions for polymer-coated silica optical fiber cannot be made because the presence or absence of the fatigue transition cannot be predicted. If the transition can be delayed beyond product design lifetimes using the strategy given in this work, then reasonable reliability predictions could be made.

Acknowledgments: We thank R. G. Huff and F. V. DiMarcello of AT&T Bell Laboratories for drawing the fiber used in this study and W. M. Russ, E. S. Chang, and J. R. Hamblin of Rutgers University for help in performing the experiments.

References

[1]S. M. Wiederhorn, "Subcritical Crack Growth in Ceramics"; pp. 613–46 in *Fracture Mechanics of Ceramics*, Vol. 2. Edited by R. C. Bradt, D. P. H. Hasselman, and F. F. Lange. Plenum Press, New York, 1974.

[2]M. J. Matthewson and C. R. Kurkjian, "Environmental Effects on the Static Fatigue of Silica Optical Fiber," *J. Am. Ceram. Soc.*, **71** [3] 177–83 (1988).

[3]J. E. Ritter, Jr., and C. L. Sherburne, "Dynamic and Static Fatigue of Silicate Glasses," *J. Am. Ceram. Soc.*, **54** [12] 601–605 (1971).

[4]G. M. Bubel and M. J. Matthewson, "Optical Fiber Reliability Implications of Uncertainty in the Fatigue Crack Growth Model," *Opt. Eng.*, **30** [6] 737–45 (1991).

[5]M. J. Matthewson, "Fiber Lifetime Predictions," *Proc. SPIE, Fiber Opt. Compon. Reliability*, **1580**, 130–41 (1991).

[6]J. T. Krause, "Transitions in the Static Fatigue of Fused Silica Fiber Lightguides," Postdeadline Paper, *Proc. Eur. Conf. Opt. Commun., 5th*, 19.11–19.14 (1979).

[7]T. T. Wang and H. M. Zupko, "Long-Term Mechanical Behaviour of Optical Fibres Coated with a UV-Curable Epoxy Acrylate," *J. Mater. Sci.*, **13**, 2241–48 (1978).

[8]J. T. Krause, "Zero Stress Strength Reduction and Transitions in Static Fatigue of Fused Silica Fiber Lightguides," *J. Non-Cryst. Solids*, **38–39**, 497–502 (1980).

[9]H. C. Chandan and D. Kalish, "Temperature Dependence of Static Fatigue of Optical Fibers Coated with a UV-Curable Polyurethane Acrylate," *J. Am. Ceram. Soc.*, **65** [3] 171–73 (1982).

[10]M. J. Matthewson, C. R. Kurkjian, and J. T. Krause, "Static Fatigue Testing of Optical Fibers," *Am. Ceram. Soc. Bull.*, **64** [3] 468 (1985); presented at the 87th Annual Meeting of the American Ceramic Society, Cincinnati, OH, May 1985 (Paper No. 14-G-85).

[11]D. Roberts, E. Cuellar, and L. M. Middleman, "Static Fatigue of Optical Fibers in Bending II: Effect of Humidity and Proof Stress on Fatigue Lifetimes," *Proc. SPIE, Symp. Fiber Opt. Integr. Optoelectron.*, **842**, 32–40 (1987).

[12]J. P. Clarkin, B. J. Skutnik, and B. D. Munsey, "Enhanced Strength and Fatigue Resistance of Silica Fibers with Hard Polymeric Coatings," *J. Non-Cryst. Solids*, **102**, 106–11 (1988).

[13]T. S. Wei and B. J. Skutnik, "Effect of Coating on Fatigue Behavior of Optical Fiber," *J. Non-Cryst. Solids*, **102**, 100–105 (1988).

[14]T. A. Michalske, W. L. Smith, and B. C. Bunker, "Fatigue Mechanisms in High-Strength Silica-Glass Fibers," *J. Am. Ceram. Soc.*, **74** [8] 1993–96 (1991).

[15]T. A. Michalske and S. W. Freiman, "A Molecular Mechanism for Stress Corrosion in Vitreous Silica," *J. Am. Ceram. Soc.*, **66** [4] 284–88 (1983).

[16]G. S. White, S. W. Freiman, S. M. Wiederhorn, and T. D. Coyle, "Effects of Counterions on Crack Growth in Vitreous Silica," *J. Am. Ceram. Soc.*, **70** [12] 891–95 (1987).

[17]W. B. Hillig and R. J. Charles, "Surfaces, Stress-Dependent Surface Reactions, and Strength"; pp. 682–705 in *High Strength Materials*. Edited by V. F. Zackay. Wiley, New York, 1965.

[18]T. Chuang and E. R. Fuller, "Extended Charles–Hillig Theory for Stress-Corrosion Cracking of Glass," *J. Am. Ceram. Soc.*, **75** [3] 540–45 (1992).

[19]C. R. Kurkjian, J. T. Krause, and U. C. Paek, "Tensile Strength Characteristics of 'Perfect' Silica Fibers," *J. Phys. (Paris)*, **43** [12] C9-585–586 (1982).

[20]R. S. Robinson and H. H. Yuce, "Scanning Tunneling Microscopy Study of Optical Fiber Corrosion: Surface Roughness Contribution to Zero-Stress Aging," *J. Am. Ceram. Soc.*, **74** [4] 814–18 (1991).

[21]H. H. Yuce, J. P. Varachi, Jr., J. P. Kilmer, C. R. Kurkjian, and M. J. Matthewson, "Optical Fiber Corrosion: Coating Contribution to Zero-Stress Aging," Postdeadline Paper PD21, *OFC'92 Tech. Digest*, 1992.

[22]D. Inniss, Q. Zhong, and C. R. Kurkjian, "Chemically Corroded Pristine Silica Fibers: Blunt or Sharp Flaws?," *J. Am. Ceram. Soc.*, in press.

[23]M. J. Matthewson, V. V. Rondinella, B. Lin, and S. W. Keyes, "The Effect of Alkali Metal Cations on the Strength and Fatigue of Fused Silica Optical Fiber," *J. Am. Ceram. Soc.*, **74** [10] 2592–98 (1991).

[24]P. W. J. G. Wijnen, T. P. M. Beelen, J. W. de Haan, C. P. J. Rummens, L. J. M. van de Ven, and R. A. van Santen, "Silica Gel Dissolution in Aqueous Alkali Metal Hydroxides Studied by ^{29}Si NMR," *J. Non-Cryst. Solids*, **109**, 85–94 (1989).

[25]V. V. Rondinella and M. J. Matthewson, "Effect of Loading Mode and Coating on Dynamic Fatigue of Optical Fiber in Two-Point Bending," *J. Am. Ceram. Soc.*, **76** [1] 139–44 (1993).

[26]"Cab-O-Sil Properties and Functions," Cabot Corp., Tuscola, IL, 1983.

[27]M. J. Matthewson and C. R. Kurkjian, "Static Fatigue of Optical Fibers in Bending," *J. Am. Ceram. Soc.*, **70** [9] 662–68 (1987).

[28]P. W. France, M. J. Paradine, M. H. Reeve, and G. R. Newns, "Liquid Nitrogen Strengths of Coated Optical Glass Fibers," *J. Mater. Sci.*, **15**, 825–30 (1980).

[29]J. T. Krause, L. R. Testardi, and R. N. Thurston, "Deviations From Linearity in the Dependence of Elongation upon Force for Fibres of Simple Glass Formers and of Glass Optical Lightguides," *Phys. Chem. Glasses*, **20** [6] 135–39 (1979).

[30]M. J. Matthewson, C. R. Kurkjian, and S. T. Gulati, "Strength Measurement of Optical Fibers by Bending," *J. Am. Ceram. Soc.*, **69** [11] 815–21 (1986).

[31]H. H. Yuce, M. E. Melczer, and P. L. Key, "Mechanical Properties of Optical Fibers in Bending," *Proc. Int. Conf. Integr. Opt., 7th*, **2**, 44 (1989).

[32]M. J. Matthewson, H. H. Yuce, V. V. Rondinella, P. R. Foy, and J. R. Hamblin, "Effect of Silica Particles in the Polymer Coating on the Fatigue and Aging Behavior of Fused Silica Optical Fiber," Postdeadline Paper PD21, *OFC/IOOC '93 Tech. Digest*, **4**, 87–90 (1993).

[33]J. Colaizzi, M. J. Matthewson, T. Iqbal, and M. R. Shahriari, "Environmental Effects on the Mechanical Properties of Aluminum Fluoride Glass Fibers," *Ceram. Trans.*, **28**, 579–86 (1992). □